Pure spin-glass resistivity maximum at the "freezing" temperature

A. W. Sheikh*
Faculty of Science, University of Garyounis, Benghazi, Libya
(Received 8 May 1989)

We have derived the pure spin-glass resistivity devoid of Kondo effect. This exhibits a broad maximum which signals the onset of the spin-glass state. As the temperature decreases towards the spin-glass freezing temperature T_f, a gradual increase in the number of "frozen" spins leads to this maximum. An expression for the ratio T_m/T_f (where T_m is the temperature for the experimental impurity resistivity maximum) has been obtained and the effects of potential scatterings have been taken into account through resonance phase shifts. Finally, we have tested various predictions of this theory with classical experimental results.

I. INTRODUCTION

Metallic spin glasses consist of magnetic impurities diluted in a noble metal (e.g., Mn, $S=\frac{5}{2}$ in Ag) and show a peak[1] in ac susceptibility at a temperature T_f. Its resistivity change (relative to the host noble metal) varies roughly linearly with temperature near T_f and has a broad maximum at a temperature T_m much higher than T_f. At low temperatures the resistivity change varies proportionally to $T^{3/2}$ (Ref. 2) or proportionally to T^2.[3] The maximum is explained in two ways: first, the Kondo effect is taken for granted, and the maximum is theoretically linked to an interplay of spin-glass properties and the Kondo effect;[4,5] second, the Kondo effect is neglected, and the maximum is explained due to the combined effect of a modified-phonon contribution ($\Delta\rho_{\rm ph}\simeq -bT$) and the Ruderman-Kittel-Kasuya-Yosida (RKKY) spin-flip scattering contribution ($\Delta\rho_{\rm RKKY}=-c/T$).[6] The low-temperature variation of the resistivity has been linked theoretically to the temperature variation of the spin-glass order parameter[7,8] and to elementary excitations in spin glasses.[9] As in experiments, none of these theories has revealed any structure signalling the onset of the spin-glass state at T_f. Since experimental data of the field-dependent ac susceptibility $\chi(H,T)=\chi_0(T)+a(T)H^2+b(T)H^4+\ldots$ do not diverge at T_f, whereas the coefficients $a(T)$ and $b(T)$, etc., reveal a power-law divergence evidencing phase transitions,[10] it is a theoretical problem to decode the resistivity data so that it also marks some kind of change at T_f. We believe that this problem requires a knowledge of the natures of the spins. In the low-temperature spin-glass phase, the Kondo effect is quenched[5] by high internal fields of frozen spins, whereas a high-temperature $\ln T$ term[2] in the observed resistivity is expected to be reminiscent of the existence of the Kondo effect. Thus spin-glass alloys contain two types of spins: effective free spins and frozen spins. The natures of frozen spins are given by Rivier and Adkins[11] (RA) according to which, impurity spins located at random, exhibit no long-range magnetic order at any temperature in spite of having its moments frozen in random orientations at low temperatures. Further RA theory models this frozen spin system as a supercooled paramagnet, i.e., the short-range order in the spin-glass phase is negligible. In a previous paper,[12] we have developed a resistivity theory of spin-glass alloys using a modified Kondo theory for effective free spins and the RA theory for frozen spins. Best fittings of the theory with experiments using free parameters have eliminated Kondo effects and yielded the pure spin-glass resistivity of frozen spins.

Here we have rederived the spin-diffusion constant Λ of RA theory in the quenched random situation, taking into account the finite mean-free paths (mfp) of conduction electrons. We have also included the resonance phase shift due to potential scatterings into the unitarity limit of RA theory. Using these modifications, we have obtained a theoretical expression for the pure spin-glass resistivity due to frozen spins. This pure spin-glass resistivity now marks the position of spin-glass freezing temperatures T_f by a rounded maximum. This maximum arises due to a progressive freezing of spins as the temperature is lowered and indicates the freezing of nearly all spins. Finally, an expression for the ratio T_m/T_f has been derived and several predictions of the theory have been tested with experiments.

II. MODEL FORMALISM

Several authors[13,14] have predicted a hole $P(H)=0$ for $-H_e\le H\le H_e$ in local-field distributions $P(H,T)$ of spin glasses whose Hamiltonian is given by[13]

$$\mathcal{H}=-\tfrac{1}{2}\sum_{i,j}J_{ij}\mathbf{S}_i\cdot\mathbf{S}_j\ ;$$

J_{ij} is for $i\neq j$ a random-exchange interaction and $J_{ii}\equiv 0$. Effective free spins lie at the lowest local field H_e and frozen spins have local fields $|H_i|>|H_e|$. Their concentrations are $X_e=X\exp(-T_m/T)$ and $X_i=Xf_i=X[1-\exp(-T_m/T)]$, respectively. Here X is the impurity concentrations and $T_m=(g\mu_B H_e)/k$.[12]

III. SPIN-DIFFUSION CONSTANT Λ OF RA THEORY

We write the diffusion constant Λ from RA theory[11] as

$$\Lambda=\frac{\pi^2}{18}\frac{a^2S}{(2K_Fa)^3}\langle J_0(a/R_{ij})^3\rangle_c f'(\lambda)\ . \tag{3.1}$$

Here the impurity concentration X is replaced by $X=\frac{1}{4}\langle(a/R_{ij})^3\rangle_c$ in case of fcc host lattice and J_0 is the strength of an infinite-ranged RKKY interaction,

$$f'(\lambda)=[(\lambda/a)^2-1]/8\ln(\lambda/a)$$

and $\langle\ \rangle_c$ represents configuration averages.

The factor $f'(\lambda)$ introduces the effect of finite mean-free path (mfp) λ of conduction electrons into the diffusion constant Λ and has been found to be in disagreement with experiments.[12] So, instead of $f'(\lambda)$, we have taken the λ effect through a damped RKKY interaction of random sign,[15]

$$J(R_{ij})\sim\pm J_0(a/R_{ij})^3 e^{-R_ij/\lambda}\ ,$$

and obtained in the quenched random situation[16]

$$\Lambda=\frac{\pi^2}{18}\frac{Sa^2k}{(2K_Fa)^3}\frac{T_f}{b_s}f(\lambda_{\rm DMR})\ , \tag{3.2}$$

where

$$T_f=b_s\frac{J^2(2l+1)^2}{4E_Fk}\sqrt{3X}\times\left[\int_1^\infty\frac{du}{u^4}e^{-\gamma u}(1-e^{X'(1-u^3)})\right]^{1/2}\ , \tag{3.3}$$

$b_s=[(2S+1)^4-1]^{1/2}/12$, l is the orbital angular momentum, and R_{ij} is the distance between spins (i) and (j). $X'=X/(1-X)$ and $\gamma=rX$. Here r is a damping factor.[16] $\lambda_{\rm DMR}$ is the mfp of conduction electrons, caused by deviations from Matthiessen's rule (DMR). The factor $f(\lambda_{\rm DMR})$ represents the DMR effect and $f(\lambda_{\rm DMR})\to1$ for $\lambda_{\rm DMR}\to\infty$.

IV. EFFECTS OF POTENTIAL SCATTERINGS

The electrostatic potential V arising from the difference in core charge between the host and the impurity atoms has been neglected in RA theory. But several authors[17,18] have reported reasonable values of V and the resistivities due to impurity potential scatterings have been estimated[18] to be 0.26, 1.20, and 2.16 $\mu\Omega$ cm for 1.1, 5.0, and 9.0 at.% Mn in Ag. In addition, we have observed[12] that the unitarity limit $\rho(\infty)$ of RA theory disagrees with experiments. These facts have encouraged us to introduce the effect of V into RA theory. In general, if the host metal is treated in the nearly-free-electron approximation, the wave functions outside the region of the impurity potential are simply phase-shifted outgoing partial waves[19] as would be expected on the basis of scattering theory. For incident conduction electron energies E far from the resonance energies E_d of spin-split virtual bound states, the phase shifts of all angular momenta l are negligible. However E near the resonance energies E_d, the particular phase shift with angular momentum l_0 of the resonant virtual bound state will be large. In the case of the transition-atom impurities $l_0=2$ and due to the spin-orbit interaction of these impurities, the $l=2$ component of the conduction electron's partial waves' angular momenta is enhanced.[20] This produces the resonance scattering for E near to E_d. Such resonance scattering has the phase shift[19]

$$\delta_r=\sum_\sigma\tan^{-1}\left[\frac{\Delta^\sigma}{E_d^\sigma-E}\right] \tag{4.1}$$

Here, Δ^σ is the width of the split virtual bound states and σ is the spin state. We have introduced this phase shift δ_r into the temperature-independent part[21] of RA theory by replacing its unitarity limit with $\rho(\infty)\sin^2\delta_r$.

V. THE PURE SPIN GLASS RESISTIVITY

We have used here RA theory to describe the resistivity of frozen spins. Briefly, this theory assumes the interaction between impurity spins to be RKKY-type and has shown[22] that the elementary excitations are spin diffusion modes. Using the multiple scattering approximation (MSA) for long wavelength excitations, Rivier and Adkins[11] have calculated

$$\Delta\rho_{\rm RA}=\rho(\infty)\left[1-\frac{D}{1+C'DT^{3/2}}\right]\ , \tag{5.1}$$

where

$$\rho(\infty)=\tfrac{1}{2}X(m/\hbar e^2)\Gamma(n/\Omega)^{-1}\ , \tag{5.2}$$

$$C'=(2\pi)^{-1}(JS/\Gamma)^2(\pi k/2\Lambda a^{-2})^{3/2}\ . \tag{5.3}$$

For a split virtual bound state of width Δ straddling the Fermi level $E_F=0$ at $\pm E_d$, D is given by

$$D=[1+(\Delta/E_d)^2]^{-1}\ . \tag{5.4}$$

D is also related to a characteristic temperature $T_{\rm ch}$ given by[12]

$$T_{\rm ch}=T_F\exp\left[-\frac{\pi^2}{\xi}\left[\frac{\Delta}{E_d}\frac{\pi}{2}\right]^{-1}\right]\ . \tag{5.5}$$

For long spin-fluctuation lifetimes, $T_{\rm ch}$ is the Kondo temperature T_K and otherwise $T_{\rm ch}=T_s=$spin-fluctuation temperature. T_F is the Fermi temperature, ξ is the s-d exchange-enhancement factor,[12] and all other symbols are as defined in RA theory.

Introducing the changes described in Secs. III and IV for the spin-diffusion constant and unitarity limit of this theory, we have derived [from Eq. (5.1)] the pure spin-glass resistivity for frozen spins of concentrations $X_i=X[1-\exp(-T_m/T)]$ as

$$\Delta\rho_{\rm SG}=A\left[1-\frac{D}{1+CDT^{3/2}f_i^{-3/4}}\right]\times[1-\exp(-T_m/T)] \tag{5.6}$$

where at

$$T=T_f,\quad X_i/(1-X_i)\simeq X/(1-X)\ , \tag{5.7}$$

$$\begin{aligned}A&=\rho(\infty)\sin^2\delta_r\\ C&=C'f_i^{3/4}\\ &=C_rT_f^{-3/2}\\ &=\tfrac{1728}{99}S^{1/2}(J/\Gamma)^2(K_Fa)^{4.5}T_f^{-3/2}b_s^{3/2}\\ &\quad\times f^{-3/2}(\lambda_{\rm DMR})\ .\end{aligned} \tag{5.8}$$

The expression (5.6) yields a broad maximum at the spin-glass freezing temperature T_f given by

$$\exp(T_m/T_f)/(T_m/T_f) = \frac{2}{3}\left[\frac{(1-D)}{C_r D^2}+\frac{(1-D)}{D}+\frac{1}{D}+C_r\right] . \quad (5.9)$$

Thus the pure spin-glass resistivity, devoid of the Kondo effect due to effective free spins, not only yields a maximum which marks the onset of the spin-glass state but also an important ratio T_m/T_f. We have detailed below several predictions of this relation (5.9), which can be tested experimentally.

(A) Pressure effect. It is well known that a change in pressure P or volume V_0 changes J and the rate of variation is given by[23]

$$\frac{d\ln|J|}{d\ln V_0} \simeq d\ln|V_{ki}|/d\ln V_0 - d\ln E_d/d\ln V_0 . \quad (5.10)$$

Here,

$$J = -|V_{ki}|^2/SE_d . \quad (5.11)$$

The covalent-admixture matrix element $|V_{ki}|^2$ is related to level width Δ of split virtual bound states as[24]

$$|V_{ki}|^2 = \frac{\Delta}{2\pi n_0(E_F)} . \quad (5.12)$$

Here, $n_0(E_F)$ is the conduction electron density of states at the Fermi level. Using Eqs. (5.4), (5.10), (5.11), and (5.12), we have derived the following relation:

$$\frac{d\ln|J|}{d\ln V_0} = \frac{d\ln(1/D-1)^{1/2}}{d\ln V_0} - \frac{2}{3} . \quad (5.13)$$

For the usual negative values of $d\ln|J|/d\ln V_0$, we have two possibilities: (i) $d\ln(1/D-1)^{1/2}/d\ln V_0$ is negative; D decreases with increasing pressures; (ii) $d\ln(1/D-1)^{1/2}/d\ln V_0$ is positive and less than $\frac{2}{3}$; D increases with increasing pressures.

Thus, we have two important predictions. (a) For large values of C_r, the ratio T_m/T_f is insensitive to the variation in D, and T_m/T_f will decrease with increasing pressure due to the dominating effect of a over J. (b) For small values of C_r, variation of D is important, and T_m/T_f will increase (decrease) in pressure due to the decrease (increase) in D.

(B) Effects of spin-orbit interactions. The s-d exchange J is enhanced by a factor ξ due to the spin-orbit coupling[12] of impurities (magnetic or nonmagnetic). Thus, the addition of impurities with strong spin-orbit coupling increases T_m/T_f.

(C) DMR effects. As resistivity due to DMR decreases [hence $f(\lambda_{\rm DMR})$ increases] with increases in X, it is predicted that C_r decreases and hence T_m/T_f decreases with increasing impurity atoms.

VI. TESTS OF THE MODEL WITH EXPERIMENTS

Resistivity maxima at T_i

In our previous papers[12,25], we have computer fitted the following expression to the resistivity data of Ford and Mydosh:[2]

$$\Delta\rho(T) = A\left[1-\frac{D}{1+CDT^{3/2}f_i^{-1/2}}\right]\times[1-\exp(-T_m/T)] + [\gamma_p-\gamma_s\ln(T^2+T_m^2)^{1/2}]\exp(-T_m/T) . \quad (6.1)$$

We have observed that the resistivity $\Delta\rho$ is not affected appreciably if power of the function f_i varies from 0 to -1. So, the parameter values for A, D, and C obtained through this best fit can describe the pure spin-glass resistivity defined by Eq. (5.6) and are shown in Table I. Using these values of A, D, CD, and T_m, we have drawn the pure spin-glass resistivity $\Delta\rho_{\rm SG}$ as shown in Fig. 1. The presence of maxima at temperatures $\simeq T_f$ confirms the theoretical prediction.

TABLE I. Best-fit parameters for Eq. (6.1) in the text, calculated values of phase shifts δ_r and the theoretical estimates of D(ps) and $\rho(\infty)$. For the evaluation of $\rho(\infty)$ and δ_r, using Eqs. (5.2) and (5.7) in the text, the following parameters have been utilized in the sequence Ag-Mn, Au-Mn, Cu-Mn: $\Gamma = 8.175$, 8.265, 9.693 eV (Ref. 12); $(n/V) = 5.85\times10^{22}$, 5.9×10^{22}, 8.5×10^{22} cm^{-3}. In the case of $E_d^{\sigma} = E_d^{-\sigma}$, $\Delta^{-\sigma} = \Delta^{\sigma} = \Delta$, and $E \simeq E_F = 0$, the theoretical calculations, D(ps) of the parameter D have been performed using Eqs. (4.1) and (5.4) and values of δ_r from this table.

Alloys	A ($\mu\Omega$ cm)	CD ($K^{-3/2}$)	D	D(ps)	δ_r	$\rho(\infty)$ ($\mu\Omega$ cm)
Ag–3.0 at. % Mn	4.954±0.003	0.600±0.002	0.800±0.003	0.87	41.5	11.293
Ag–5.4 at. % Mn	8.789±0.005	0.538±0.013	0.813±0.008	0.88	41.0	20.327
Ag–5.9 at. % Mn	9.591±0.002	0.589±0.009	0.899±0.005	0.88	41.0	22.210
Ag–9.7 at. % Mn	15.670±0.007	0.496±0.018	0.817±0.025	0.88	41.0	36.514
Au–1.5 at. % Mn	3.848±0.001	3.808±0.394	0.870±0.085	0.77	57.0	5.482
Au–2.8 at. % Mn	6.670±0.007	1.250±0.093	0.900±0.005	0.79	54.0	10.233
Au–4.6 at. % Mn	11.286±0.001	0.819±0.003	0.875±0.005	0.79	55.0	16.812
Au–7.7 at. % Mn	18.162±0.007	0.400±0.001	0.870±0.001	0.79	54.0	28.142
Cu–2.7 at. % Mn	8.299±0.001	1.267±0.133	0.828±0.023		90.0	8.299
Cu–4.5 at. % Mn	12.650±0.005	1.000±0.038	0.900±0.015		73.0	13.832
Cu–6.3 at. % Mn	17.295±0.002	0.800±0.004	0.900±0.044		70.9	19.364

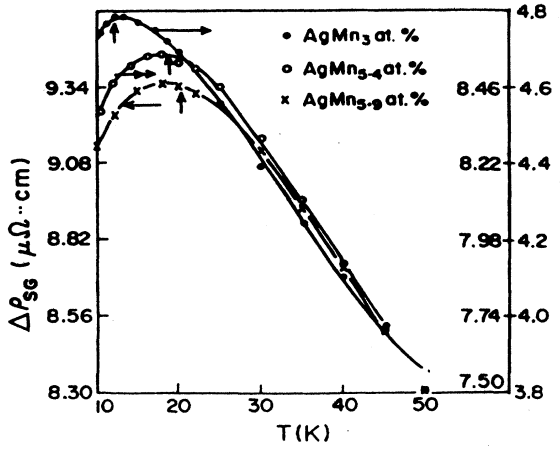

FIG. 1. The pure spin-glass resistivity is plotted against temperature. The double arrow points to the inner right-hand scale. Vertical arrows indicate the positions of freezing temperatures T_f.

The ratio T_m/T_f

In Table II theoretical estimates $(T_m/T_f)_{\text{th}}$ of the ratio T_m/T_f shown within brackets ( ) are very close to its calculations using parameters derived from experiments. We have also listed the experimental values $(T_m/T_f)_{\text{ex}}$ of the ratio T_m/T_f in Table II. Notwithstanding the variations of T_m/T_f with impurity concentrations due to DMR effects,[2] our theoretical results $(T_m/T_f)_{\text{th}}$ shown within brackets ( ) agree reasonably well with $(T_m/T_f)_{\text{ex}}$.

In a remarkable way, our theoretical estimates $(T_m/T_f)_{\text{th}}$ provide an answer to the hitherto unexplained results of high $(T_m/T_f)_{\text{ex}}$ in Au-Mn compared to Au-Cr with the same impurity concentrations in the same host. Furthermore, we have measured $T_m = 132$ and 178 X for $Y = 0.05$ and 0.10, respectively, in $(Cu_{1-Y}Pd_Y)Mn_{0.10}$. This is in agreement with the prediction of the effects of spin-orbit interactions on T_m/T_f, since the spin-orbit scatterer also increases T_f.[26] Details are reserved for future work.

TABLE II. Experimental values of T_f, T_m and $(T_m/T_f)_{\text{ex}}$ and the estimates of $(T_m/T_f)_{\text{th}}$, C_r, and D(th). For the evaluation of C_r, using Eq. (5.8) with $f(\lambda_{\text{DMR}})=1$, the following parameters have been utilized in the sequence Ag-Mn, Au-Mn, Cu-Mn, and Au-Cr: $S=1.95\pm0.1$ (Ref. 26), 2.25 ± 0.1 (Ref. 26), 2.05 (Ref. 27), 1.0; $J=0.184$, 0.157, 0.213, 0.176 eV (Ref. 23); $\xi=1.43$, 1.36, 1.5 (Ref. 12); $n_0(E_F)=0.262$, 0.308, 0.294, 0.308 eV^{-1} (Ref. 23); $T_K=10^{-4}$, 10^{-4}, 0.012, 0.001 K (Ref. 23); $\Gamma=kT_K\exp[1/n_0(E_F)|J|]=8.8$, 8.3, 8.9, 8.9 eV; $K_F=1.20$, 1.20, 1.36, 1.20 Å^{-1}; $T_F=6.36\times10^4$, 6.39×10^4, 8.12×10^4, 6.39×10^4 K; $a=4.09$, 4.08, 3.61, 4.08 Å. The theoretical values D(th) of the parameter D have been calculated from Eqs. (5.4) and (5.5) in the text, using values of T_F, T_K, and ξ cited above. Finally, best-fit values of C and D from Table I and experimental values of T_f from this table have been utilized to find theoretical estimates $(T_m/T_f)_{\text{th}}$ of the ratio T_m/T_f, using Eqs. (5.8) and (5.9). Also, we have calculated $(T_m/T_f)_{\text{th}}$ from Eq. (5.9) in the text and using values of C_r and D(th) from this table. These are listed separately within ( ).

Alloys	T_f(K)	T_m(K)	$(T_m/T_f)_{\text{ex}}$	$(T_m/T_f)_{\text{th}}$	C_r	D(th)
Ag–0.6 at. % Mn	3.4	47	13.8	(5.75)		
Ag–1.1 at. % Mn	5.5	43	7.8			
Ag–3.0 at. % Mn	12	64	5.33	4.65	79.17	0.80
Ag–5.4 at. % Mn	19	90	4.74	5.30		
Ag–5.9 at. % Mn	20.5	95	4.63	5.40		
Ag–9.7 at. % Mn	30	130	4.33	6.0		
Au–0.5 at. % Mn	3.5	60	17.0	(5.80)		
Au–1.5 at. % Mn	7.0	75	10.7	5.80		
Au–2.8 at. % Mn	11	85	7.7	5.20	77.03	0.87
Au–4.6 at. % Mn	16.5	105	6.36	5.45		
Au–7.7 at. % Mn	25	125	5.0	5.35		
Au–11.8 at. % Mn	34	150	4.4			
Cu–0.7 at. % Mn	8	17	5.63	(6.20)		
Cu–1.6 at. % Mn	13	45	3.46			
Cu–2.7 at. % Mn	18	70	3.89	6.20	132.14	0.83
Cu–4.5 at. % Mn	27	100	3.70	6.50		
Cu–6.3 at. % Mn	33	144	4.36	7.20		
Cu–9.7 at. % Mn	44	190	4.38			
Au–0.9 at. % Cr	14	35	2.50			
Au–1.5 at. % Cr	22	47	2.14	(2.40)	5.58	0.90
Au–3.3 at. % Cr	35	85	2.40			
Au–4.9 at. % Cr	50	100	2.0			
Au–7.9 at. % Cr	78	150	1.92			
Au–10.6 at. % Cr	100	185	1.80			

Pressure effects on T_m/T_f

Cu-Mn, Au-Fe. In these two systems[29,30] $dT_f/dP>0$, whereas $dT_m/dP\simeq 0$ for Cu-Mn and $dT_m/dP<0$ for Au-Fe. Thus, the ratio T_m/T_f decreases with increasing pressures in both cases.

Au-Mn, Ag-Mn. For both of these alloys,[30] $dT_f/dP>0$ and also[29] $dT_m/dP>0$. We have estimated in Au–0.10 at. % Mn,[29] $dT_m/dP=1.838$ mK/kbar, and in Au–3 at. % Mn,[30] $dT_f/dP=25.5\pm 3.5$ mK/kbar. Since dT_f/dP is independent of impurity concentrations according to[30]

$$d(\ln T_f)/dV_0=2d\ln|J|/dV_0+d\ln n_0(E_F)/dV_0\ , \qquad (6.2)$$

we have $dT_m/dP<dT_f/dP$ and hence the ratio T_m/T_f decreases with increasing pressures. Thus, experimental results on all these four systems Cu-Mn, Au-Fe, Au-Mn, and Ag-Mn confirm the prediction (A) of the expression (5.9).

Au-Cr system. Since,[30]

$$\frac{d\ln|J|}{d\ln V_0}(\mathrm{Au-Fe})\simeq\frac{d\ln|J|}{d\ln V_0}(\mathrm{Au-Cr})\ ,$$

we have[30] $(dT_f/dP)_{\mathrm{Au-Cr}}\simeq(dT_f/dP)_{\mathrm{Au-Fe}}=(15.5\pm 2.5)$ mK/kbar. Also, we have evaluated,[31] $dT_m/dP=-0.51$, 0.0, and 1.4 mK/kbar for 0.10, 0.15, and 0.3 at. % Cr in Au, respectively. This gives $dTm/dP=9.42X$ mK/kbar, where X is the concentration of Cr in at. %. Thus $dT_m/dP<dT_f/dP$ for $X<1.7$ and $dT_m/dP>dT_f/dP$ for $X>1.7$. This means that the predictions (A) and (B) of the expression (5.9) are confirmed in the same system Au-Cr with low and high concentrations, respectively. We suggest pressure experiments in Au-Cr of high-impurity concentrations and also in Pd-Cr to test prediction (B).

Phase-shift δ_r.

In the case of Ag-Mn,[32] $E_d^{\sigma}=-3.1\pm 0.2$ eV, $E_d^{-\sigma}=2.1\pm 0.2$ eV, $\Delta^{\sigma}=0.7\pm 0.1$ eV, $\Delta^{-\sigma}=1.2\pm 0.1$ eV. So Ag-Mn and probably Au-Mn also approach the ideal case of a split virtual bound state (vbs) of width Δ straddling the Fermi level ($E_F=0$) at $\pm E_d$, and we have shown theoretical estimates D (ps) of D for these two systems in Table I. The values of D(ps) are in fair agreement with best-fit values of D.

In case of Cu-Mn, the energy E_d of minority spin state is far away from the energy E_d of majority spin state. Assuming $\Delta^{\sigma}\simeq\Delta^{-\sigma}=\Delta$ and using Eqs. (4.1) and (5.4), we have calculated the ratio $|E_d^{\sigma}/E_d^{-\sigma}|$ from the best-fit values of D and δ_r listed in Table I. For 2.7, 4.5, and 6.3 at. % Mn in Cu, the estimated values of $|E_d^{\sigma}/E_d^{-\sigma}|$ are 4.13, 4.22, and 3.92. Theoretically reported value of $|E_d^{\sigma}/E_d^{-\sigma}|$ in Cu-Mn (Ref. 32) is 4.375. Thus our results are in good agreement with the theory.

VII. CONCLUSIONS

We have obtained the pure spin-glass resistivity devoid of Kondo effect. This exhibits a maximum at the freezing temperature T_f. The pure spin-glass resistivity obtained through the best-fit parameters of the theory with experiments yields a maximum at $T\simeq T_f$ in agreement with the model. Several aspects of an expression of the ratio T_m/T_f have been tested successfully with experiments. The resonance phase shift δ_r introduced into the unitarity limit of RA theory also finds satisfactory agreements with experiments. The population of frozen spins $X_i=X[1-\exp(-T_m/T)]$ continuously builds up as the temperature is decreased, and at $T=T_f$ nearly all spins are frozen. Thus it is a progressive type of freezing rather than a cooperative freezing, while effective free spins undergo a cooperative freezing at T_f.[33]

*Permanent address: 12 P.P. Rd, New Delhi-110001, India.

[1]V. Cannela and J. A. Mydosh, Phys. Rev. B **6**, 4220 (1972).
[2]P. J. Ford and J. A. Mydosh, Phys. Rev. B **14**, 2057 (1976).
[3]O. Laborde and P. Radhakrishna, J. Phys. F **3**, 1731 (1973).
[4]U. Larsen, Phys. Rev. B **14**, 4356 (1976); **18**, 5014 (1978).
[5]K. H. Fischer, Z. Phys. B **42**, 27 (1981).
[6]Fu-sui, Liu, W. R. Roshen, and J. Ruvalds, Phys. Rev. B **36**, 492 (1987).
[7]J. Seiden, C. R. Acad. Sci. Ser. B **282**, 149 (1976).
[8]F. S. Huang, J. Appl. Phys. **53**, 7705 (1982).
[9]I. A. Campbell, P. J. Ford and A. Hamzic, Phys. Rev. B **26**, 5195 (1982).
[10]E. Zastre, R. M. Roshko, and Gwyn Williams, Phys. Rev. B **32**, 7597 (1985).
[11]N. Rivier and K. Adkins, J. Phys. F **5**, 1745 (1975).
[12]A. W. Sheikh, J. Phys. F **18**, 2015 (1988).
[13]A. J. Bray and M. A. Moore, J. Phys. C **14**, 2629 (1981).
[14]G. S. Grest and C. M. Soukoulis, Phys. Rev. B **28**, 2886 (1983).
[15]U. Larsen, Phys. Rev. B **33**, 4803 (1986).
[16]U. Larsen, Solid State Commun. **22**, 311 (1977).
[17]M. T. Beal-Monod and R. A. Weiner, Phys. Rev. **170**, 552 (1968).
[18]W. C. Kok, Phys. Lett. **55A**, 187 (1975).
[19]A. J. Heeger, Solid State Phys. **23**, 296 (1969).
[20]S. M. Goldberg, P. M. Levy, and A. Fert, Phys. Rev. B **33**, 276 (1986).
[21]J. Kondo, Solid State Phys. **23**, 262 (1969).
[22]N. Rivier, Wiss. Z. Techn. Univ. Dresden **23**, 1000 (1974).
[23]J. S. Schilling, Adv. Phys. **28**, 657 (1979).
[24]R. Podloucky, R. Zeller, and P. H. Doderichs, Phys. Rev. B **22**, 5777 (1980).
[25]A. W. Sheikh and M. El-Fazani, Phys. Status Solidi B **147**, 601 (1988).
[26]F. W. Smith, Solid State Commun. **25**, 341 (1978).
[27]A. F. J. Morgownik and J. A. Mydosh, Solid State Commun. **47**, 321 (1983).
[28]G. S. Sherlekar, C. M. Srivastava, S. Ramakrishnan, and G. Chandra, Phys. Rev. B **38**, 720 (1988).

[29]J. S. Schilling, P. J. Ford, U. Larsen, and J. A. Mydosh, Phys. Rev. B **14**, 4368 (1976).
[30]U. Hardebusch, W. Garhardt, and J. S. Schilling, Z. Phys. B **60**, 463 (1985).
[31]J. Willer, J. Crone, and E. Luscher, J. Phys. F **9**, 2411 (1979).
[32]D. van der Marel, G. A. Sawatzky, and F. U. Hillebrecht, Phys. Rev. Lett. **53**, 1206 (1984).
[33]A. W. Sheikh, Phys. Lett. A **132**, 276 (1988).